

Article

Ferrotorryweiserite, $Rh_5Fe_{10}S_{16}$, a New Mineral Species from the Sisim Placer Zone, Eastern Sayans, Russia, and the Torryweiserite–Ferrotorryweiserite Series

Andrei Y. Barkov ^{1,*}, Nadezhda D. Tolstykh ², Nobumichi Tamura ³ , Robert F. Martin ⁴, Andrew M. McDonald ⁵ and Louis J. Cabri ⁶

- ¹ Research Laboratory of Industrial and Ore Mineralogy, Cherepovets State University, 5 Lunacharsky Avenue, 162600 Cherepovets, Russia
 - ² V.S. Sobolev Institute of Geology and Mineralogy, Siberian Branch of the Russian Academy of Science, 3 Avenue Prospekt Koptuyuga, 630090 Novosibirsk, Russia; tolst@igm.nsc.ru
 - ³ Advanced Light Source, Lawrence Berkeley National Laboratory, 1 Cyclotron Road, Berkeley, CA 94720-8229, USA; ntamura@lbl.gov
 - ⁴ Department of Earth and Planetary Sciences, McGill University, 3450 University Street, Montreal, QC H3A 0E8, Canada; robert.martin@mcgill.ca
 - ⁵ Harquail School of Earth Sciences, Laurentian University, 935 Ramsey Lake Road, Sudbury, ON P3E 2C6, Canada; amcdonald@laurentian.ca
 - ⁶ Cabri Consulting Inc., 514 Queen Elizabeth Drive, Ottawa, ON K1S 3N4, Canada; lcabri@outlook.com
- * Correspondence: ore-minerals@mail.ru; Tel.: +7-820-255-65-97



Citation: Barkov, A.Y.; Tolstykh, N.D.; Tamura, N.; Martin, R.F.; McDonald, A.M.; Cabri, L.J. Ferrotorryweiserite, $Rh_5Fe_{10}S_{16}$, a New Mineral Species from the Sisim Placer Zone, Eastern Sayans, Russia, and the Torryweiserite–Ferrotorryweiserite Series. *Minerals* **2021**, *11*, 1420. <https://doi.org/10.3390/min11121420>

Academic Editor: Evgeny Galuskin

Received: 29 October 2021

Accepted: 10 December 2021

Published: 15 December 2021

Publisher's Note: MDPI stays neutral with regard to jurisdictional claims in published maps and institutional affiliations.



Copyright: © 2021 by the authors. Licensee MDPI, Basel, Switzerland. This article is an open access article distributed under the terms and conditions of the Creative Commons Attribution (CC BY) license (<https://creativecommons.org/licenses/by/4.0/>).

Abstract: Ferrotorryweiserite, $Rh_5Fe_{10}S_{16}$, occurs as small grains ($\leq 20 \mu\text{m}$) among droplet-like inclusions (up to $50 \mu\text{m}$ in diameter) of platinum-group minerals (PGM), in association with oberthürite or Rh-bearing pentlandite, laurite, and a Pt-Pd-Fe alloy (likely isoferroplatinum and Fe-Pd-enriched platinum), hosted by placer grains of Os-Ir alloy ($\leq 0.5 \text{ mm}$) in the River Ko deposit. The latter is a part of the Sisim placer zone, which is likely derived from ultramafic units of the Lysanskiy layered complex, southern Krasnoyarskiy kray, Russia. The mineral is opaque, gray to brownish gray in reflected light, very weakly bireflectant, not pleochroic to weakly pleochroic (grayish to light brown tints), and weakly anisotropic. The calculated density is $5.93 \text{ g}\cdot\text{cm}^{-3}$. Mean results (and ranges) of four WDS analyses are: Ir 18.68 (15.55–21.96), Rh 18.34 (16.32–20.32), Pt 0.64 (0.19–1.14), Ru 0.03 (0.00–0.13), Os 0.07 (0.02–0.17), Fe 14.14 (13.63–14.64), Ni 13.63 (12.58–14.66), Cu 4.97 (3.42–6.41), Co 0.09 (0.07–0.11), S 29.06 (28.48–29.44), and total 99.66 wt.%. They correspond to the following formula calculated for a total of 31 atoms per formula unit: $(Rh_{3.16}Ir_{1.72}Pt_{0.06}Ru_{0.01}Os_{0.01})_{\Sigma 4.95}(Fe_{4.48}Ni_{4.11}Cu_{1.38}Co_{0.03})_{\Sigma 10.00}S_{16.05}$. The results of synchrotron micro-Laue diffraction studies indicate that ferrotorryweiserite is trigonal; its probable space group is $R\bar{3}m$ (#166) based on its Ni-analog, torryweiserite. The unit-cell parameters refined from 177 reflections are $a = 7.069$ (2) Å, $c = 34.286$ (11) Å, $V = 1484$ (1) Å³, and $Z = 3$. The $c:a$ ratio is 4.8502. The strongest eight peaks in the X-ray diffraction pattern derived from results of micro-Laue diffraction study [d in Å(hkl)(I)] are 2.7950 (2025) (100); 5.7143 (0006) (60); 1.7671 (2240) (44.4); 3.0486 (2021) (39.4); 5.7650 (1012) (38.6); 2.5956 (2027) (37.8); 3.0058 (1126) (36.5); and 1.5029 (42 212) (35.3). Ferrotorryweiserite and the associated PGM crystallized from microvolumes of residual melt at late stages of crystallization of grains of Os- and Ir-dominant alloys occurred in lode zones of chromitites of the Lysanskiy layered complex. In a particular case, the residual melt is disposed peripherally around a core containing a disequilibrium association of magnesian olivine ($For_{72.9-75.6}$) and albite ($Ab_{81.6-86.4}$), with the development of skeletal crystals of titaniferous augite: $Wo_{40.8-43.2}En_{26.5-29.3}Fs_{20.3-22.6}Aeg_{6.9-9.5}$ (2.82–3.12 wt.% TiO_2). Ferrotorryweiserite represents the Fe-dominant analog of torryweiserite. We also report occurrences of ferrotorryweiserite in the Marathon deposit, Coldwell Complex, Ontario, Canada, and infer the existence of the torryweiserite–ferrotorryweiserite solid solution in other deposits and complexes.

Keywords: ferrotorryweiserite; torryweiserite–ferrotorryweiserite solid solution; platinum-group mineral; PGE sulfide; rhodium–iron sulfide; olivine–plagioclase inclusions; Sisim placer zone; River Ko deposit; Lysanskiy layered complex; Eastern Sayans; Russia

1. Introduction

Ferrotorryweiserite, $Rh_5Fe_{10}S_{16}$, is a new mineral species discovered in the River Ko suite, which represents part of the Sisim placer zone, south of Krasnoyarsk, Krasnoyarskiy kray, Russia (approximate location $54^{\circ}45' N$, $93^{\circ}09' E$). The mineral and its name were approved (IMA 2021-055) by the Commission on New Minerals, Nomenclature and Classification (CNMNC) of the International Mineralogical Association [1]. Our aims are to describe its properties and to report, with reference to literature sources, on the probable existence of a complete solid-solution series between ferrotorryweiserite and torryweiserite, $Rh_5Ni_{10}S_{16}$, discovered in the Marathon Cu–Pd deposit, Coldwell complex, Ontario, Canada [2–4]. Ferrotorryweiserite is also related to tamuraite, $Ir_5Fe_{10}S_{16}$, and kuvaevite, $Ir_5Ni_{10}S_{16}$ [5,6], which are other members of the torryweiserite family that also occur as inclusions in grains of Os–Ir alloy in heavy-mineral fractions of platinum-group minerals (PGM) in the placer zone of the Sisim river and its tributaries, rivers Ko and Seyba [7,8]. An evaluation of the economic potential of these placers had not yet been completed. The placer grains of PGM were likely derived from ultramafic units of the Lysanskiy layered complex, Eastern Sayans, south-central Siberia [9]. In relation to the series of ferrotorryweiserite–torryweiserite, we document an unusual occurrence of the association olivine–albite (For_{73-76} and Ab_{82-86}) developed in the core of a globular inclusion hosted by a grain of iridium from the River Ko. Additional occurrences of members of the ferrotorryweiserite–torryweiserite series are expected in a variety of ore deposits associated with ultramafic–mafic complexes that are known to contain Rh- and Ir-based species of PGM, cf. [10,11].

2. Materials and Methods

Hundreds of grains of Os–Ir alloy minerals and inclusions were examined from placer suites in the Sisim zone. In some of these grains from the River Ko, ferrotorryweiserite occurs as composite inclusions in other PGM hosted by osmium enriched in Ir or, less commonly and inversely, by iridium enriched in Os.

Electron-microprobe analyses of ferrotorryweiserite and iridium were done at McGill University by means of wavelength spectrometry (WDS) using a JEOL JXA 8900L facility operated at 20 kV, 20 nA, with a beam diameter set at 3 μm . The following X-ray lines were used: $CuK\alpha$, $NiK\alpha$, $FeK\alpha$, $CoK\alpha$, $IrL\alpha$, $RhL\alpha$, $PtL\alpha$, $PdL\beta$, $OsM\alpha$, $RuL\alpha$, and $SK\alpha$. Counting times were 20 s on the peak. The Phi–Rho–Z method of corrections was applied. The peak-overlap corrections included $Fe \rightarrow Co$, $Os \rightarrow Ir$, $Ru \rightarrow Pd$, $Ir \rightarrow Pt$, and $Ru \rightarrow Rh$ corrections. The standards used are pure metals for the platinum-group elements (PGE), Fe, Cu, Co, and pentlandite for Ni and S. Values of standard deviations (σ) are ≤ 0.2 wt.% for Ir, Pt, and Cu, ≤ 0.1 wt.% for Ru, Os, Fe, and Ni, and ≤ 0.05 wt.% for Rh, Co, and S.

The minerals were also analyzed via quantitative energy-dispersive spectrometry (EDS), at 20 kV and 1.6 nA, using a MIRA 3 LMU (Tescan Orsay Holding, Brno, Czech Republic) scanning electron microscope with an attached INCA Energy 450 XMax 80 (Oxford Instruments Nanoanalysis, Wycombe, UK) system at the Analytical Center for multi-elemental and isotope studies, SB RAS, Novosibirsk, Russia. The following X-ray lines were used: $SiK\alpha$, $TiK\alpha$, $AlK\alpha$, $CrK\alpha$, $MgK\alpha$, $FeK\alpha$, $NaK\alpha$, $KK\alpha$, $CuK\alpha$, $NiK\alpha$, $CoK\alpha$, $IrL\alpha$, $RhL\alpha$, $PtL\alpha$, and $SK\alpha$. Minimum detection limits (2σ level) are ≤ 0.2 wt.% for S, Fe, Co, Ni, Cu; ≤ 0.4 wt.% for Rh; and ≤ 0.5 – 0.7 wt.% for Ir. Certified standards were used, such as pure metals, SiO_2 , TiO_2 , Al_2O_3 , Cr_2O_3 , and FeS_2 , along with diopside, albite, and orthoclase. The analytical error for the main components did not exceed 1–2 relative %.

Synchrotron micro-Laue diffraction studies, followed by monochromator energy scans, were performed on the holotype specimens of ferrotorryweiserite at the Advanced Light Source (ALS) of the Lawrence Berkeley National Laboratory, Berkeley, CA, USA. The Laue diffraction patterns were collected using a PILATUS 1M area detector operated in reflection geometry. The patterns were analyzed and indexed using the software package XMAS v.6 after Tamura, 2014 [12].

3. Results and Observations

3.1. Appearance, Properties, and Morphology

Ferrotorryweiserite occurs as small grains ($\leq 20 \mu\text{m}$), which are portions of composite, droplet-like inclusions (up to 50–70 μm in diameter) of PGM, mainly oberthürite or pentlandite enriched in Rh, laurite, Pt-(Pd)-Fe alloy (isoferroplatinum or Fe-Pd-rich platinum), braggite-vysotskite, vasilite, and chalcopyrite, hosted by placer grains of Os- or Ir-dominant Os-Ir alloys ($\leq 0.5 \text{ mm}$ across) (Figures 1 and 2a,b). In general, the PGM assemblage is dominated by Os-Ir-Ru alloys, where osmium is a major species, and iridium is subordinate. Rutheniridosmine is rare. The compositional field is limited to the Ru-poor portion of the system Os–Ir–Ru by the line Ru:Ir = 1 in the entire Sisim–Ko–Seyba placer area [9]. In addition, ferrotorryweiserite has also been observed in the Marathon deposit, Coldwell Complex, Ontario, Canada, in association with torryweiserite and oberthürite, $\text{Rh}_3(\text{Ni,Fe})_{32}\text{S}_{32}$ [3].

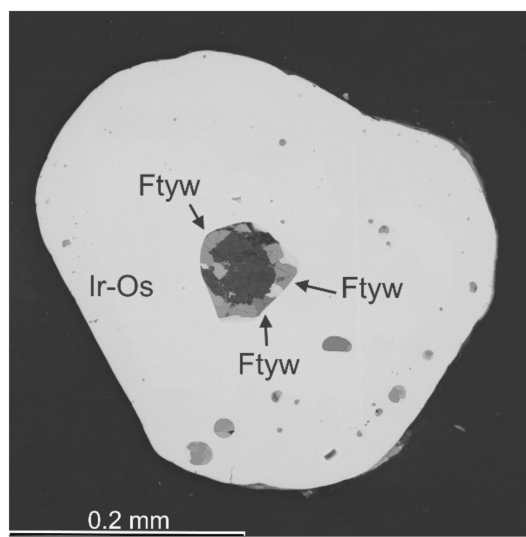


Figure 1. A backscattered electron image (BSE) showing a rounded, subhedral grain of iridium enriched in Os (labeled Ir-Os) which hosts globular or elongate inclusions of PGE- and base-metal sulfides (gray in the BSE) from the River Ko placer. An intermediate member of the ferrotorryweiserite–torryweiserite series (labeled Ftyw) occurs as a portion of a composite and partial rim deposited around an olivine-plagioclase core (dark gray in the BSE), which includes skeletal forms of titaniferous augite. The host is epoxy. See Figure 2b–d for greater magnification and details.

Ferrotorryweiserite develops as anhedral grains; no evidence of twinning was observed. The $c:a$ ratio calculated from the unit-cell parameters is 4.8502.

In reflected light, ferrotorryweiserite is gray to brownish gray. Bireflectance is very weak to absent. The mineral is not pleochroic or weakly pleochroic (gray to light brown tints). It is weakly anisotropic (gray to light yellow tints). Internal reflections were not observed; neither reflectance values nor streak could be examined because of the small grain sizes. The mineral is opaque; its luster is metallic. Fluorescence and tenacity were not determined, and hardness values (Mohs or micro-indentation) could not be measured owing to the small grain size. No cleavage or fracture were observed. The density also could not be measured. The calculated value of density, $5.93 \text{ g}\cdot\text{cm}^{-3}$, is based on the unit-

cell volume (1484 \AA^3) derived from diffraction measurements by means of synchrotron radiation and the empirical formula.

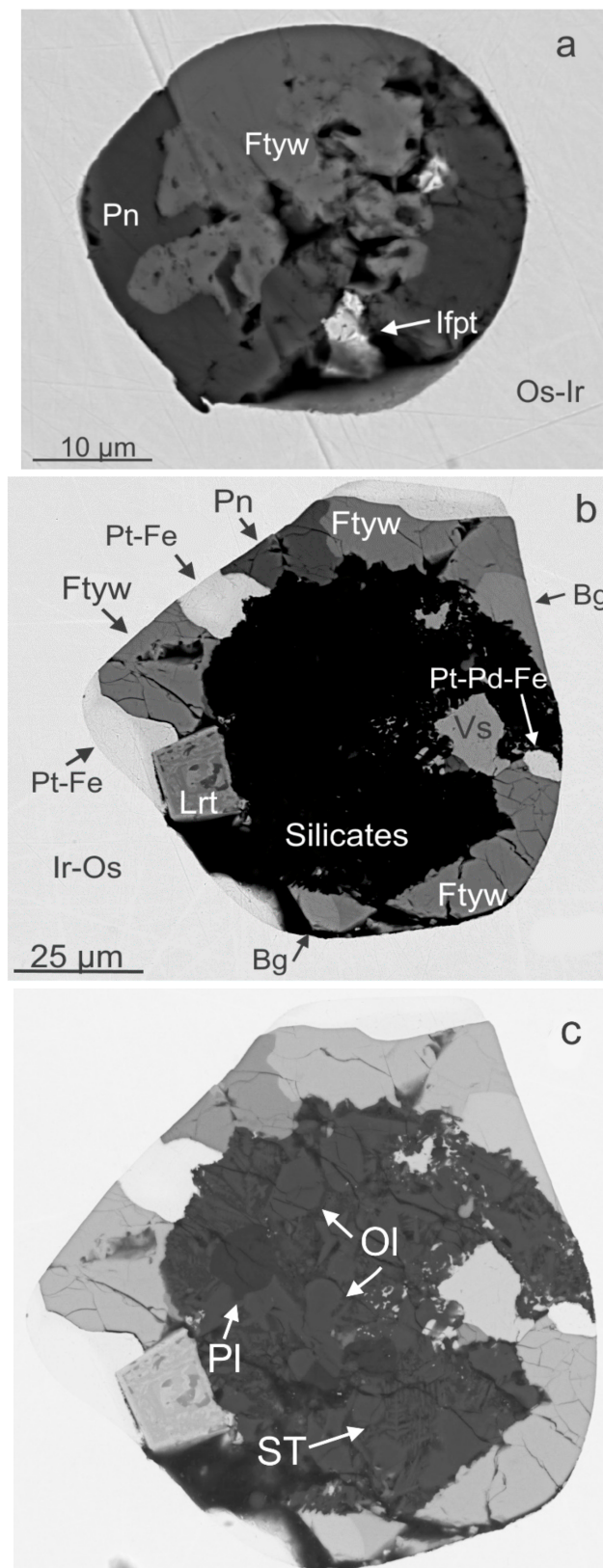


Figure 2. Cont.

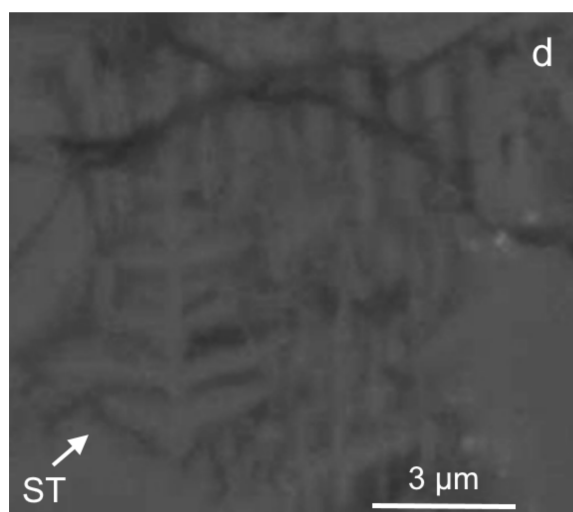


Figure 2. BSE images showing characteristic examples of droplet-like inclusions of platinum-group minerals (a,b) hosted by placer grains of Os-Ir alloys, which correspond to osmium or iridium (labeled Os-Ir and Ir-Os, respectively). Grains of ferrotorreyweiserite (Ftyw), shown in (a), and inclusions of an intermediate member of the ferrotorreyweiserite–torreyweiserite series (b) are associated with oberthürite or Rh-rich pentlandite (Pn), a Pt-Fe alloy (possibly isoferroplatinum, Ifpt) or with related alloys of Pt-Fe and Pt-(Pd)-Fe compositions (labeled Pt-Fe and Pt-Pd-Fe), braggite-vysotskite (Bg), vasilite (Vs), and laurite (Lrt). Note the presence of an unusual intergrowth of silicate minerals (black in the BSE), which is composed of olivine (Ol; Fo_{73-76}) and subordinate amounts of sodic plagioclase, Pl (Ab_{82-86}), developed in the core of the globular inclusion shown in Figures 1 and 2b. Forms with a skeletal texture (ST) are observed locally in the silicate core (b–d), which is composed of titaniferous augite ($\text{Wo}_{40.8-43.2}\text{En}_{26.5-29.3}\text{Fs}_{20.3-22.6}\text{Aeg}_{6.9-9.5}$). The scale bar and symbols, relevant to (c), are shown in (b).

3.2. Mineral Association and Compositions

The silicate core, mantled by the rim-like aggregate of grains of ferrotorreyweiserite–torreyweiserite and other PGM (Figures 1 and 2b,c), is composed mainly of microgranular olivine, Fo_{73-76} , with a subordinate quantity of sodic plagioclase enriched in albite: Ab_{82-86} (Table 1). The skeletal texture (Figures 1 and 2b–d) is formed by lamellar grains of titaniferous augite (2.82–3.12 wt.% TiO_2) enriched in the aegirine component: $\text{Wo}_{41-43}\text{En}_{27-29}\text{Fs}_{20-23}\text{Aeg}_{7-10}$, which is less magnesian ($\text{Mg}\#$ 53.8–59.3; $\text{Mg}\# = 100 \text{ Mg} / (\text{Mg} + \text{Fe}^{2+} + \text{Mn})$) than the olivine.

Table 1. Compositions of olivine, clinopyroxene, and plagioclase in the core of globular inclusion hosted by the grain of Ir-Os alloy in the River Ko area.

wt.%	Ol-1	Ol-2	Ol-3	Ol-4	Cpx	Pl-1	Pl-2	Apfu	Ol-1	Ol-2	Ol-3	Ol-4	Cpx	Pl-1	Pl-2
SiO ₂	37.93	38.21	38.74	38.68	47.24	66.17	67.71	Si	1.00	1.01	1.00	1.01	1.72	2.96	2.95
TiO ₂	0	0	0	0	3.12	0	0	Ti	0	0	0	0	0.09	0	0
Al ₂ O ₃	0	0	0	0	13.17	19.99	20.39	Al	0	0	0	0	0.57	1.05	1.05
FeO	20.80	23.02	21.23	22.62	10.81	0	0.40	Fe	0.46	0.51	0.46	0.50	0.33	0	0.01
MnO	0.37	0.32	0	0.30	0	0	0	Mn	0.01	0.01	0	0.01	0	0	0
MgO	38.59	36.85	39.19	37.01	8.74	0.22	0	Mg	1.51	1.45	1.51	1.44	0.48	0	0
CaO	0.38	0.43	0.56	0.55	17.91	2.10	2.32	Ca	0.01	0.01	0.02	0.02	0.70	0.10	0.11
NiO	0.62	0.56	0.60	0.61	0	0	0	Ni	0.01	0.01	0.01	0.01	0	0	0
Na ₂ O	0	0	0	0	1.58	9.15	9.07	Na	0	0	0	0	0.11	0.79	0.77
K ₂ O	0	0	0	0	0.11	0.43	0.57	K	0	0	0	0	0.01	0.02	0.03
Total	98.69	99.39	100.32	99.77	102.68	98.06	100.46	Fo (An)	75.6	72.9	75.6	73.2	-	11.0	12.0
								Fa (Ab)	22.8	25.5	23.0	25.1	-	86.4	84.6
								Tep (Or)	0.4	0.4	0	0.3	-	2.7	3.5

Note: Results of quantitative energy-dispersive X-ray spectrometry (EDS) obtained in conjunction with scanning electron microscopy (SEM) are listed in weight %. Zero means “below detection”. Values of atoms per formula unit (apfu) are based on four oxygen atoms for olivine (Ol), six atoms for clinopyroxene (Cpx), and eight atoms for plagioclase (Pl). Values of end-member components are expressed in mol %, i.e., forsterite (Fo), fayalite (Fa), and tephroite (Tep) in olivine, and anorthite (An), albite (Ab), and orthoclase (Or) in plagioclase.

Various species of PGM and base-metal sulfides were recognized in association with ferrotorreyweiserite: braggite-vysotskite, vasilite, laurite, oberthürite, or Rh-rich pentlandite, Pt-(Pd)-Fe alloys, and chalcopyrite (Table 2). Our compositions are consistent with pentlandite, corresponding to the general formula $Rh(Ni_4Fe_4)S_8$ or $(Rh, Co, Pd)(Ni_4Fe_4)S_8$, in which one atom per formula unit of Rh + Pd + Co likely enters a distinct site.

Table 2. Compositions of ore minerals associated with ferrotorreyweiserite in the River Ko placer area.

#	Mineral	S	Fe	Co	Ni	Cu	Ru	Rh	Ir	Os	Pt	Pd	Total, wt. %
1	Bg-1	22.60	0.32	0	3.84	0	0	0	0	0	7.68	64.44	98.88
2	Bg-2	22.50	0.33	0	3.74	0	0	0	0	0	8.13	64.46	99.16
3	Vs	11.68	1.62	0	0	3.62	0	0	0	0	0	82.19	99.11
4	Lrt-1	33.18	0.51	0	0.50	0	35.89	0	4.01	27.38	0	0	101.47
5	Lrt-2	37.16	0.35	0	0.46	0	53.04	0	4.88	4.03	0	0	99.92
6	Lrt-3	36.75	0.38	0	0.44	0	55.13	0	1.90	3.34	0	0	97.94
7	Lrt-4	37.14	0.48	0	0.73	0	52.51	0	6.41	4.79	0	0	102.06
8	Pn-1	30.93	25.10	0	28.37	0	0	11.72	0	0	0	0	96.12
9	Pn-2	31.36	25.25	0	28.26	0	0	11.78	0	1.28	0	0	97.93
10	Pn-3	31.71	30.31	0.93	25.96	0	0	7.21	0	0	0	1.65	97.77
11	Ccp	34.48	29.19	0	0.37	32.91	0	0	0	0	0	0	96.95
12	Pt-Fe alloy-1	0	12.33	0	0.84	0	0	0	0	0	61.72	21.13	96.02
13	Pt-Fe alloy-2	0	11.78	0	0.67	0	0	0	0	0	62.52	22.62	97.59
14	Pt-Fe alloy-3	0	10.05	0	0.52	0	0	0	0	0	87.14	2.29	100.00
15	Pt-Fe alloy-4	0	12.12	0	2.23	0	0	0	6.34	0	72.98	0.99	96.00
16	Pt-Fe alloy-5	0	11.88	0	1.00	0.85	0	0	0	0	68.77	13.91	96.41
17	Ir-dominant alloy	0	0.33	0	0.02	0	1.19	0.74	59.97	35.12	2.00	0.14	99.50
18	Os-Ir alloy-1	0	0	0	0.42	0	8.95	0	35.42	56.11	0	0	100.90
19	Os-Ir alloy-2	0	0	0	0	0	6.88	0	42.63	51.48	0	0	100.99

<i>Atoms per formula unit (apfu)</i>												
#	S	Fe	Co	Ni	Cu	Ru	Rh	Ir	Os	Pt	Pd	
1	0.99	0.01	0	0.09	0	0	0	0	0	0.06	0.85	
2	0.99	0.01	0	0.09	0	0	0	0	0	0.06	0.85	
3	6.85	0.55	0	0	1.07	0	0	0	0	0	14.53	
4	1.97	0.02	0	0.02	0	0.68	0	0.04	0.27	0	0	
5	1.99	0.01	0	0.01	0	0.90	0	0.04	0.04	0	0	
6	1.98	0.01	0	0.01	0	0.94	0	0.02	0.03	0	0	
7	1.98	0.01	0	0.02	0	0.89	0	0.06	0.04	0	0	
8	8.15	3.80	0	4.08	0	0	0.96	0	0	0	0	
9	8.18	3.78	0	4.03	0	0	0.96	0	0.06	0	0	
10	8.10	4.45	0.13	3.62	0	0	0.57	0	0	0	0.13	
11	2.03	0.99	0	0.01	0.98	0	0	0	0	0	0	
12	0	29.44	0	1.91	0	0	0	0	0	42.18	26.47	
13	0	27.92	0	1.51	0	0	0	0	0	42.43	28.14	
14	0	27.38	0	1.36	0	0	0	0	0	67.98	3.28	
15	0	32.32	0	5.66	0	0	0	4.91	0	55.72	1.39	
16	0	29.29	0	2.35	1.84	0	0	0.00	0	48.53	18.00	
17	0	1.12	0	0.05	0	2.20	1.34	58.49	34.62	1.92	0.25	
18	0	0	0	1.24	0	15.40	0	32.05	51.30	0	0	
19	0	0	0	0	0	12.15	0	39.57	48.28	0	0	

Note: Results of quantitative SEM-EDS analyses (#1–16, 18, 19) and wavelength-dispersive X-ray spectrometry (WDS; #17) are listed in weight %. Zero means “below detection”. The atomic proportions are based on a total of 2 apfu for braggite-vysotskite, Bg (#1, 2), 23 apfu for vasilite, Vs (#3), 3 apfu for laurite, Lrt (#4–7), 17 apfu for oberthürite or Rh-rich pentlandite, Pn (#8–10), and 4 apfu for chalcopyrite, Ccp (#11). Compositions of Pt-(Pd)-Fe alloys (#12–16), iridium rich in Os (#17), and osmium rich in Ir (#18, 19) were recalculated based on a total of 100 at %. A minor amount of S (1.34 wt.%), present in analysis #15, is ascribed to interference from the associated sulfide. The slightly lower totals observed in some of the analyses are attributed to an insufficient volume of the grains.

3.3. Chemical Composition and Formula of Ferrotorreyweiserite

Mean results of electron-microprobe analyses (WDS) of four grains of ferrotorreyweiserite, each based on four data-points ($n = 4$; Table 3), correspond to the following formula based on a total of 31 atoms per formula unit (apfu) by analogy and according to the structure of the Ni-dominant analog, i.e., torreyweiserite [3]: $(Rh_{3.16}Ir_{1.72}Pt_{0.06}Ru_{0.01}Os_{0.01})_{\Sigma 4.95}(Fe_{4.48}Ni_{4.11}Cu_{1.38}Co_{0.03})_{\Sigma 10.00}S_{16.05}$.

Table 3. Chemical data for ferrotorryweiserite from the River Ko placer deposit.

Constituent	Mean (wt.%) WDS *	Range (wt.%)	Mean (wt.%) EDS **	Range (wt.%)
Cu	4.97	3.42–6.41	6.18	6.01–6.43
Ni	13.63	12.58–14.66	12.46	11.18–12.90
Fe	14.14	13.63–14.64	13.52	13.24–14.18
Co	0.09	0.07–0.11	0	0
Ir	18.68	15.55–21.96	17.67	15.39–25.05
Rh	18.34	16.32–20.32	19.06	13.46–20.95
Pt	0.64	0.19–1.14	0.34	0–1.72
Os	0.07	0.02–0.17	0	0
Ru	0.03	0–0.13	0	0
S	29.06	28.48–29.44	29.00	27.82–29.45
Total	99.66		98.23	

Note: * Results of WDS analyses; ** Results of quantitative SEM/EDS analyses. The mean values of WDS and EDS analyses are based on four and five data points, respectively. Zero means “not detected”.

Results of quantitative SEM/EDS analyses performed on additional grains of ferrotorryweiserite ($n = 5$; Table 3) are also in agreement, leading to $(\text{Rh}_{3.31}\text{Ir}_{1.64}\text{Pt}_{0.03})_{\Sigma 4.98}(\text{Fe}_{4.33}\text{Ni}_{3.79}\text{Cu}_{1.74})_{\Sigma 9.86}\text{S}_{16.16}$. The simplified formula is $(\text{Rh},\text{Ir})_5(\text{Fe},\text{Ni},\text{Cu})_{10}\text{S}_{16}$. Consequently, the ideal formula, $\text{Rh}_5\text{Fe}_{10}\text{S}_{16}$, based on the assumption that other elements are not essential, requires Rh 32.44, Fe 35.21, and S 32.34, total 100 wt.%.

The average of four WDS data points, carried out on specimens of ferrotorryweiserite from the Marathon deposit, Coldwell complex, Ontario, Canada, gives the formula $(\text{Rh}_{4.59}\text{Ir}_{0.11}\text{Pt}_{0.06})_{\Sigma 4.76}(\text{Fe}_{4.62}\text{Ni}_{3.58}\text{Cu}_{1.66}\text{Co}_{0.39})_{\Sigma 10.24}\text{S}_{15.99}$. A total value of all metals is notably stoichiometric (15 *apfu*) in this formula. Thus, a minor amount of a Fe-site cation is presumably present at the Rh site.

Compositional variations documented in the ferrotorryweiserite–torryweiserite series in the River Ko placer area are presented in Table 4. Compositions of grains of ferrotorryweiserite from other complexes and ore deposits are listed in Table 5.

Table 4. Compositions of members of the ferrotorryweiserite–torryweiserite series from the River Ko placer area.

#	S	Fe	Co	Ni	Cu	Ru	Rh	Ir	Os	Pt	Total, wt.%
2	28.48	14.64	0.09	14.66	3.65	0.00	16.32	21.96	0.02	0.19	100.02
3	28.96	14.33	0.11	14.54	3.42	0.00	16.78	21.46	0.02	0.30	99.91
4	29.44	13.63	0.07	12.58	6.41	0.00	19.96	15.55	0.17	1.14	98.96
5	29.38	13.97	0.07	12.74	6.40	0.13	20.32	15.75	0.07	0.94	99.77
6	31.20	13.58	0.12	18.74	2.62	0.01	29.32	4.24	0.00	0.11	99.95
7	30.81	13.43	0.14	18.74	2.53	0.04	29.40	4.50	0.00	0.24	99.83
8	30.69	13.33	0.12	18.95	2.18	0.03	28.99	4.30	0.03	0.34	98.95
9	31.00	13.23	0.12	18.49	1.90	0.32	30.99	4.00	0.00	0.04	100.09
10	31.06	13.40	0.11	18.88	2.29	0.04	29.65	4.45	0.00	0.35	100.23
11	28.78	12.31	0.09	15.66	4.04	0.07	16.76	20.83	0.03	0.88	99.45
12	28.31	12.45	0.09	16.20	3.77	0.06	16.61	20.65	0.07	0.79	99.00
13	27.95	12.09	0.08	16.08	3.80	0.05	16.49	20.93	0.06	1.09	98.63
14	30.68	13.20	0.13	18.46	2.15	0.44	30.14	4.191	0.00	0.15	99.53
15	28.80	9.70	0.05	16.37	7.15	0.03	17.93	17.94	0.04	1.91	99.92
16	28.59	9.56	0.05	16.36	6.80	0.02	17.58	17.89	0.08	2.04	98.95
17	29.97	13.63	0.04	14.60	6.43	0.05	23.97	10.58	0.01	0.75	100.03
18	30.00	13.09	0.05	14.85	6.30	0.01	23.93	10.57	0.00	0.62	99.42

<i>Apfu</i> (based on a total of 31 <i>apfu</i>)													
#	S	Fe	Co	Ni	Cu	Ru	Rh	Ir	Os	Pt	ΣPGE	$\Sigma(\text{Fe},\text{Ni},\text{Cu},\text{Co})$	ΣMe
1	15.99	4.55	0.03	4.53	0.99	0.00	2.85	2.04	0.00	0.02	4.91	10.10	15.01
2	15.89	4.69	0.03	4.47	1.03	0.00	2.84	2.04	0.00	0.02	4.90	10.21	15.11
3	16.10	4.57	0.03	4.41	0.96	0.00	2.91	1.99	0.00	0.03	4.92	9.98	14.90

Table 4. Cont.

Apfu(based on a total of 31 apfu)													
#	S	Fe	Co	Ni	Cu	Ru	Rh	Ir	Os	Pt	ΣPGE	Σ(Fe,Ni,Cu,Co)	ΣMe
4	16.17	4.30	0.02	3.77	1.78	0.00	3.42	1.42	0.02	0.10	4.96	9.87	14.83
5	16.04	4.38	0.02	3.80	1.76	0.02	3.46	1.43	0.01	0.08	5.00	9.96	14.96
6	15.99	4.00	0.03	5.25	0.68	0.00	4.68	0.36	0.00	0.01	5.06	9.95	15.01
7	15.90	3.98	0.04	5.28	0.66	0.01	4.73	0.39	0.00	0.02	5.14	9.96	15.10
8	15.94	3.97	0.04	5.38	0.57	0.01	4.69	0.37	0.00	0.03	5.10	9.96	15.06
9	15.98	3.91	0.03	5.20	0.49	0.05	4.98	0.34	0.00	0.00	5.38	9.65	15.02
10	15.96	3.95	0.03	5.30	0.59	0.01	4.75	0.38	0.00	0.03	5.16	9.88	15.04
11	16.12	3.96	0.03	4.79	1.14	0.01	2.92	1.95	0.00	0.08	4.97	9.92	14.88
12	15.95	4.02	0.03	4.98	1.07	0.01	2.92	1.94	0.01	0.07	4.95	10.11	15.05
13	15.91	3.95	0.03	5.00	1.09	0.01	2.92	1.99	0.01	0.10	5.03	10.07	15.09
14	15.92	3.93	0.04	5.23	0.56	0.07	4.87	0.36	0.00	0.01	5.32	9.76	15.08
15	15.99	3.09	0.02	4.96	2.00	0.01	3.10	1.66	0.00	0.17	4.94	10.07	15.01
16	16.03	3.08	0.01	5.01	1.92	0.00	3.07	1.67	0.01	0.19	4.94	10.02	14.97
17	15.91	4.15	0.01	4.23	1.72	0.01	3.96	0.94	0.00	0.07	4.97	10.12	15.09
18	15.99	4.00	0.01	4.32	1.69	0.00	3.97	0.94	0.00	0.05	4.97	10.03	15.01

Note: These results of WDS analyses are listed in weight %, and values of atoms per formula unit (apfu) are based on a total of thirty-one atoms per formula unit (apfu). Zero means “not detected”. Analyses #1–5 pertain to ferrotorreyweiserite, and #6–18 correspond to torreyweiserite.

Table 5. Compositions of grains of ferrotorreyweiserite from other localities.

Locality	Marathon			Tulameen			Yubdo			Miass		Mean
	1	2	3	4	5	6	7	8	9	10		
wt.%												
S	32.63	31.38	30.49	31.82	30.07	31.90	32.10	31.80	31.90	28.22	31.23	
Fe	21.05	14.00	14.55	13.90	16.83	16.30	15.80	15.60	17.80	14.94	16.08	
Co	0.75	2.20	0.66	2.10	0.00	1.01	1.09	1.11	0.80	0.00	1.22	
Ni	10.17	14.57	12.51	14.45	9.96	11.50	11.60	11.60	10.10	12.52	11.90	
Cu	5.75	6.44	7.12	6.64	5.78	4.71	4.34	4.05	4.71	3.32	5.29	
Ru	0.00	0.00	0.00	0.00	0.04	0.00	0.00	0.00	0.00	0.00	0.04	
Rh	28.77	30.39	25.59	31.65	20.95	27.20	27.40	28.20	26.50	17.14	22.07	
Ag	0.03	0.00	0.00	0.00	0.00	0.00	0.00	0.00	0.00	0.00	0.03	
Ir	0.00	0.00	5.34	0.06	18.20	6.81	6.70	6.54	7.21	22.96	9.23	
Os	0.00	0.00	0.00	0.05	0.15	0.00	0.00	0.00	0.00	0.00	0.10	
Pt	0.21	0.19	2.13	0.33	1.24	0.96	1.20	1.05	0.70	0.00	0.89	
Total, wt.%	99.36	99.17	98.39	101.00	103.22	100.39	100.23	99.95	99.72	99.10	100.05	
apfu												
S	16.16	15.86	16.06	15.88	16.10	16.42	16.55	16.49	16.48	16.06	16.20	
Fe	5.99	4.06	4.40	3.98	5.17	4.82	4.68	4.64	5.28	4.88	4.79	
Co	0.20	0.61	0.19	0.57	0.00	0.28	0.31	0.31	0.23	0.00	0.34	
Ni	2.75	4.02	3.60	3.94	2.91	3.23	3.27	3.29	2.85	3.89	3.38	
Cu	1.44	1.64	1.89	1.67	1.56	1.22	1.13	1.06	1.23	0.95	1.38	
Ru	0.00	0.00	0.00	0.00	0.01	0.00	0.00	0.00	0.00	0.00	0.01	
Rh	4.44	4.79	4.20	4.92	3.50	4.36	4.40	4.56	4.26	3.04	4.25	
Ag	0.00	0.00	0.00	0.00	0.00	0.00	0.00	0.00	0.00	0.00	0.00	
Ir	0.00	0.00	0.47	<0.01	1.63	0.59	0.58	0.57	0.62	2.18	0.83	
Os	0.00	0.00	0.00	<0.01	0.01	0.00	0.00	0.00	0.00	0.00	0.01	
Pt	0.02	0.02	0.18	0.03	0.00	0.00	0.00	0.00	0.00	0.00	0.06	
Total apfu	31.00	31.00	31.00	31.00	30.89	30.92	30.90	30.91	30.94	31.00	31.24	
ΣPGE (+Ag)	4.46	4.80	4.80	4.80	5.14	4.95	4.98	5.12	4.89	5.22	4.88	
ΣPGE/ΣMe	14.84	15.14	14.89	14.97	14.79	14.50	14.35	14.43	14.47	14.94	14.71	
Ni/Fe	0.46	0.99	0.99	0.99	0.56	0.67	0.70	0.71	0.54	0.80	0.74	
Fe/Ni	2.18	1.01	1.22	1.01	1.78	1.49	1.43	1.41	1.85	1.25	1.51	

Note: Minerals of ferrotorreyweiserite composition are from the Marathon deposit, Coldwell complex, Ontario, Canada [2–4], the Tulameen Alaskan-type complex, British Columbia, Canada, after Aubut, 1979 [13], the Yubdo placer deposit in Ethiopia after Evstigneeva, 1992 [14], and the Miass placer zone, southern Urals, Russia, after Barkov et al., 2018 [15].

3.4. Crystallography and Results of Synchrotron Micro-Laue Diffraction Study

A standard single-crystal study could not be conducted because of the small size of the grains. Thus, we have performed a synchrotron X-ray study, which also is a single-crystal diffraction technique, of ferrotorryweiserite grains analyzed by Laue microdiffraction at the 12.3.2 beam line of the Advanced Light Source (ALS). The Laue diffraction patterns were collected using a PILATUS 1M area detector operated in reflection geometry. The patterns were indexed and analyzed using XMAS v.6 (Tamura, 2014) [12]. Monochromator energy scans were used to determine the unit-cell parameters and to evaluate the basic symmetry features of ferrotorryweiserite.

Our results indicate that the mineral is trigonal, and the probable space group, $R\bar{3}m$ (#166), is inferred by analogy with the Ni-dominant analog, i.e., torryweiserite from the Marathon deposit, Coldwell complex, Ontario, Canada [2,3]. The unit-cell parameters obtained are $a = 7.069$ (2) Å, $c = 34.286$ (11) Å, $V = 1484$ (1) Å³, and $Z = 3$.

The X-ray powder-diffraction pattern derived for ferrotorryweiserite from results of synchrotron micro-Laue diffraction study (based on principles described in [12]) is listed in Table 6 together with the observed pattern for torryweiserite (IMA2020-048) from the Marathon deposit, Coldwell complex, Ontario, Canada [3]. The characteristics of ferrotorryweiserite are compared with those of related species in Table 7. Based on these results, it is inferred that ferrotorryweiserite is isostructural with torryweiserite. By analogy with the structural motif and assignments presented for torryweiserite by McDonald et al., 2021 [3], the crystal structure of ferrotorryweiserite is composed of three distinct layers of polyhedra stacked along [001]. The first is a layer of Rh1S₆ octahedra sharing edges; it has octahedral voids, such as are found in dioctahedral micas. The second is a mixed layer composed of Rh2S₆ octahedra, Fe1S₄, and Fe2S₄ tetrahedra arranged in a pinwheel fashion, with Rh2S₆ at the center. The third layer consists of a double sheet of Fe3S₄ tetrahedra that share edges along [001] to form six-membered Fe3S₄ rings. Thus, the structure is related to that of synthetic Cu₄Sn₇S₁₆ [16]. It is described in detail and illustrated in the article on torryweiserite [3].

Table 6. X-ray powder-diffraction data (d in Å) for ferrotorryweiserite.

Indices				Ferrotorryweiserite *		Torryweiserite **			
h	k	i	l	d (Å)	I	d_{obs} (Å)	d_{calc} (Å)	I_{obs}	I_{calc}
0	0	0	3	11.4287	10.0				
1	0	$\bar{1}$	2	5.7650	38.6		5.758		6
0	0	0	6	5.7143	60.8		5.712		12
1	1	$\bar{2}$	0	3.5343	10.7	3.566	3.530	17	14
2	$\bar{1}$	$\bar{1}$	3	3.3765	20.2				
2	0	$\bar{2}$	1	3.0486	39.4	3.080	3.045	33	37
1	1	$\bar{2}$	6	3.0058	36.5	3.029	3.003	58	100
1	0	$\bar{1}$	10	2.9914	21.3		2.990		51
2	0	$\bar{2}$	5	2.7950	100	2.817	2.792	23	60
2	0	$\bar{2}$	7	2.5956	37.8				
2	$\bar{1}$	$\bar{1}$	9	2.5910	6.3				
2	0	$\bar{2}$	8	2.4909	21.5	2.508	2.488	17	14
3	$\bar{1}$	$\bar{2}$	1	2.2929	12.3				
0	0	0	15	2.2857	8.6		2.282		5
2	0	$\bar{2}$	10	2.2833	22.4				
1	0	$\bar{1}$	14	2.2738	8.3				
2	0	$\bar{2}$	11	2.1839	15.6	2.199	2.182	21	23
3	$\bar{1}$	$\bar{2}$	7	2.0920	12.6				
3	0	$\bar{3}$	3	2.0087	9.8				
3	0	$\bar{3}$	6	1.9217	6.2	1.9329	1.9195	30	25
0	0	0	18	1.9048	6.2		1.9039		7
2	2	$\bar{4}$	0	1.7671	44.4	1.7797	1.7650	100	77

Table 6. Cont.

Indices			Ferrotorryweiserite *			Torryweiserite **			
<i>h</i>	<i>k</i>	<i>i</i>	<i>l</i>	<i>d</i> (Å)	<i>I</i>	<i>d</i> _{obs} (Å)	<i>d</i> _{calc} (Å)	<i>I</i> _{obs}	<i>I</i> _{calc}
2	0	$\bar{2}$	16	1.7554	9.1		1.7542		70
3	$\bar{1}$	$\bar{2}$	13	1.7393	7.2				
4	$\bar{2}$	$\bar{2}$	6	1.6882	7.5				
2	0	$\bar{2}$	17	1.6841	28.3	1.6929	1.6830	9	9
3	$\bar{1}$	$\bar{2}$	14	1.6818	20.3				
4	0	$\bar{4}$	1	1.5545	1.3				
0	2	$\bar{2}$	19	1.5290	5.0	1.5380	1.5270	12	5
1	3	$\bar{4}$	10	1.5243	8.9				
3	0	$\bar{3}$	15	1.5223	2.2		1.5199		12
4	$\bar{2}$	$\bar{2}$	12	1.5029	35.3				
4	0	$\bar{4}$	5	1.4936	11.3				
3	1	$\bar{4}$	11	1.4910	2.7		1.4920		10
4	$\bar{2}$	$\bar{2}$	15	1.3980	8.0				
2	3	$\bar{5}$	5	1.3750	1.5				
4	0	$\bar{4}$	11	1.3738	5.1		1.3723		5
2	0	$\bar{2}$	23	1.3402	8.3				
4	1	$\bar{5}$	6	1.3008	4.8				
3	2	$\bar{5}$	10	1.2997	1.7	1.3072	1.2992	23	18
4	$\bar{2}$	$\bar{2}$	18	1.2955	7.4				
4	0	$\bar{4}$	16	1.2454	23.8	1.2512	1.2442	49	21
4	0	$\bar{4}$	17	1.2191	5.6				
2	2	$\bar{4}$	21	1.1992	7.5				
1	1	$\bar{2}$	27	1.1951	2.2		1.1982		12
4	2	$\bar{6}$	1	1.1563	1.3				
3	3	$\bar{6}$	6	1.1539	1.5	1.1598	1.1517	17	17
1	3	$\bar{4}$	22	1.1481	3.50				

Note: Only reflections with $I \geq 5$ are listed. * The PXRD pattern of ferrotorryweiserite derived from results of synchrotron micro-Laue diffraction study. ** The PXRD pattern of torryweiserite after McDonald et al. [3].

Table 7. Comparison of ferrotorryweiserite to related species.

#	Species	Type Locality	Ideal Formula	Unit-Cell Parameters	Reference
1	Ferrotorryweiserite	River Ko deposit, Sisim placer zone, southwestern Eastern Sayans, Russia	Rh ₅ Fe ₁₀ S ₁₆	$a = 7.069$ (2) Å $c = 34.286$ (11) Å $V = 1484$ (1) Å ³ and $Z = 3$	(This study)
2	Torryweiserite	Marathon deposit, Coldwell complex, Ontario, Canada	Rh ₅ Ni ₁₀ S ₁₆	$a = 7.060$ (1) Å, $c = 34.271$ (7) Å, $V = 1479.3$ (1) Å ³ , and $Z = 3$	McDonald et al., 2021 [3]
3	Tamuraite	River Ko deposit	Ir ₅ Fe ₁₀ S ₁₆	$a = 7.073$ (1) Å $c = 34.277$ (8) Å $V = 1485$ (1) Å ³ and $Z = 3$	Barkov et al., 2021 [5]
4	Kuvaevite	River Ko deposit	Ir ₅ Ni ₁₀ S ₁₆	$a = 7.079$ (5) Å $c = 34.344$ (12) Å $V = 1490$ (2) Å ³ and $Z = 3$	IMA2020-043 [6]

Note: Unit-cell parameters refined from 177 reflections indexed for the ferrotorryweiserite grain (Rh_{3.46}Ir_{1.43}Pt_{0.08}Ru_{0.02}Os_{0.01})_{Σ5.00}(Fe_{4.38}Ni_{3.80}Cu_{1.76}Co_{0.02})_{Σ9.96}S_{16.04} studied by synchrotron micro-Laue diffraction. The space group $R\bar{3}m$ (#166) is inferred for these compounds by analogy with torryweiserite [3].

3.5. Name and Type Material

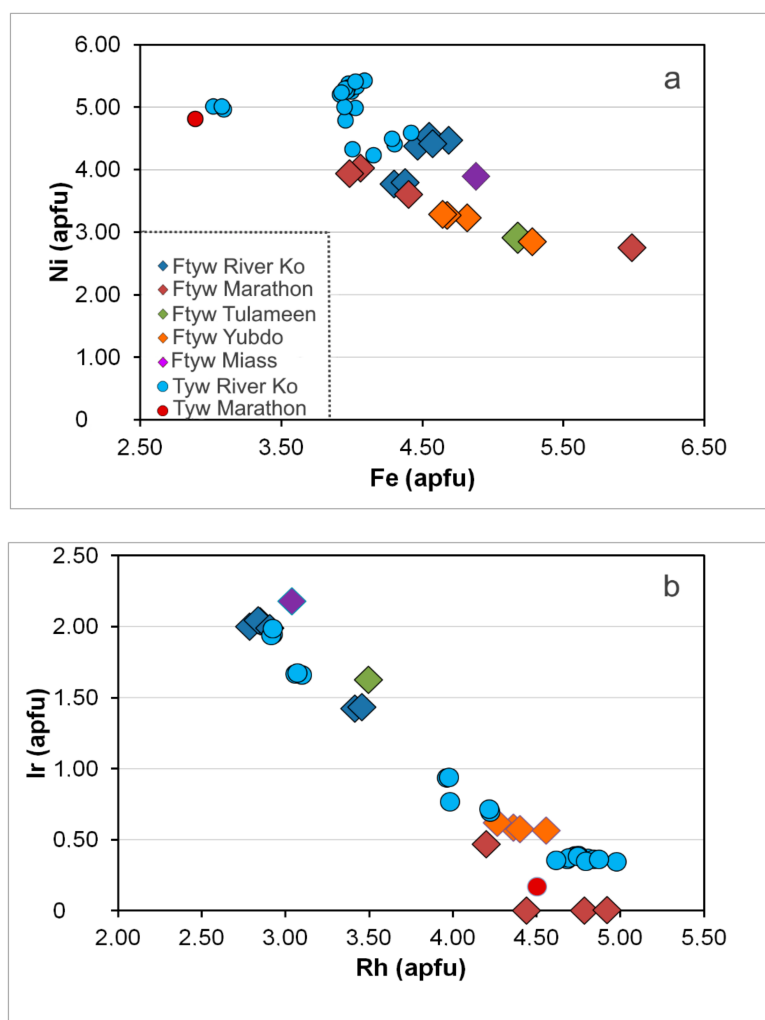
The name ferrotorryweiserite reflects its Fe-dominant composition as an analog of torryweiserite.

The holotype specimen of ferrotorryweiserite is deposited (catalog number: III-105/1) at the Central Siberian Geological Museum, Sobolev Institute of Geology and Mineralogy, Akademik Koptyug Avenue, no. 3, 630090 Novosibirsk, Russia.

4. Discussion

4.1. Relation to Other Species

As noted, ferrotorryweiserite $\text{Rh}_5\text{Fe}_{10}\text{S}_{16}$ is isostructural with torryweiserite $\text{Rh}_5\text{Ni}_{10}\text{S}_{16}$ [3] found at its type locality, the Marathon deposit, Coldwell complex, Ontario, Canada. Ferrotorryweiserite is the Fe-dominant analog of torryweiserite and is considered to form a complete series of solid solution with torryweiserite (Figure 3a,b; Tables 4 and 5). Therefore, ferrotorryweiserite belongs to the torryweiserite family of sulfide minerals, which includes tamuraite $\text{Ir}_5\text{Fe}_{10}\text{S}_{16}$ [5] and kuvaevite $\text{Ir}_5\text{Ni}_{10}\text{S}_{16}$ [6] (Table 7), all of which crystallize in space group $R\bar{3}m$ (#166).



Ferrotorreyweiserite is distinct from oberthürite ($\text{Rh}_3\text{Ni}_{32}\text{S}_{32}$), both compositionally and structurally; the latter is a member of the pentlandite group (with $a = 10.066(5)$ Å) first described from the Marathon deposit, Canada [3]. Ferrotorreyweiserite also differs from ferhodsite $[(\text{Fe},\text{Rh},\text{Ir},\text{Ni},\text{Cu},\text{Co},\text{Pt})_{9-x}\text{S}_8]$ described from Nizhniy Tagil, Urals. The latter mineral has a tetragonal unit-cell ($P42/n$ or $P4/nmm$) with parameters $a = 10.009(5)$ and $c = 9.840(8)$ Å [17]; in addition, note the critical comments in [18].

4.2. Genetic Implications and the Ferrotorreyweiserite–Torreyweiserite Series

The inferred terrane affinities and mineral associations indicate that the placer PGM grains with inclusions of the ferrotorreyweiserite–torreyweiserite solid solution are related to zones of chromitite within ultramafic units of the Lysanskiy layered complex of dunite–peridotite–gabbro. Indeed, detrital grains of chromian spinel (up to 16.6 wt.% MgO in magnesiochromite) are associated with PGM grains in the Sisim placer zone.

This complex is the likely primary source for the PGM-bearing placers for the entire Sisim placer zone. The direct intergrowths of PGM with an REE mineral, monazite-(Ce), documented at Sisim [9], resemble examples of atypical mineralization reported from the Oktyabrsky deposit, Norilsk complex, Russia [19]. Heterogeneous micro-inclusions rich in Ti, documented in the placer grains of PGM, are consistent with the inferred provenance related to the Lysanskiy complex, which is known to contain reserves of titanium [9]. The Ti-enriched composition of augite (Table 1) is notably consistent.

Members of the ferrotorreyweiserite–torreyweiserite series associated with the tamuraite–kuvaevite solid solution likely formed at an advanced stage of crystallization because of the buildup in sulfur in droplets of incompatible residual melt enriched in Ni, Fe, Cu, Rh, and lithophile elements during the formation of the alloys in lode zones of chromitites in the Lysanskiy layered complex, Eastern Sayans.

The extent of Fe-for-Ni substitution is determinative for members of the inferred ferrotorreyweiserite–torreyweiserite series (Figure 3a,b), as is reflected in data for related PGM from the River Ko placer, Eastern Sayans, Russia (this study), the Marathon deposit, Coldwell complex, Ontario, Canada [3], the Tulameen Alaskan-type complex, British Columbia, Canada [13], the Yubdo placer deposit in Ethiopia [14,20], and the Miass placer zone, southern Urals, Russia [15].

A plot of Fe vs. Ni (Figure 3a) shows a negative correlation ($R = -0.73$), calculated for Fe vs. Ni and based on a total of 39 data points available for members of the series, which contain substantial Cu. The Rh vs. Ir correlation is inverse ($R = -0.97$ for $n = 39$; Figure 3b). Note that correlations of Fe vs. Rh, Fe vs. Ir, Ni vs. Rh, and Ni vs. Ir all are statistically insignificant. Thus, the observed substitutions of Fe vs. Ni and Rh vs. Ir operate independently in the structure, and the PGE occupy crystallographic sites different from those of Ni+Fe. This is corroborated by crystal-chemical considerations reported for the type specimen of torreyweiserite from the Marathon deposit, Coldwell complex, Ontario, Canada [3].

4.3. The Olivine-Plagioclase Inclusion and Its Significance

We describe the occurrence of a highly unusual core in a globular inclusion hosted by the Ir-Os alloy (Figures 1 and 2b–d). It is composed of microgranular olivine, subordinate amounts of sodic plagioclase, and skeletal or lamellar grains of titaniferous augite. These silicates are rimmed by an intermediate member of the ferrotorreyweiserite–torreyweiserite solid solution, oberthürite or Rh-enriched pentlandite, laurite, vasilite, braggite-vysotskite, and other species.

There is a remote similarity with parageneses of olivine and plagioclase known in inclusions in carbonaceous chondrites, i.e., POIs [21] or, e.g., with the olivine-anorthite melt inclusions present in allivalite of the low-K tholeiitic island-arc series of the Kuril-Kamchatka island, Russia [22]. On the other hand, note that the association in the globule hosted by iridium differs drastically by its high enrichment in Na (Ab_{82-86}), which clearly cannot have resulted from an equilibrium crystallization with olivine of the Fo_{73-76} compo-

sition. Thus, we infer metastable conditions of crystallization with effects of overcooling, which are consistent with the development of skeletal crystals of titaniferous augite in the core (Figure 2d).

Interestingly, the sulfide phases were deposited along the periphery and around the silicate core, thus indicating a highly efficient differentiation and fractionation of sulfur and ore components, PGE, Cu-Ni-Fe, in the late portion of residual melt crystallizing after the silicate globule. Laurite, inferred to be a result of magmatic crystallization, e.g., [23], occurs in the intimate association with palladium species, such as braggite-vysotskite (Figure 2b), which formed under submagmatic conditions, cf. [24]. These observations are consistent with the hydrothermal origin of laurite, as inferred in the Imandra complex, Russia [25], and could well imply a similarly low-temperature crystallization of laurite, ferrotorryweiserite, and associated species in the ore assemblage deposited in the rim assemblage.

The overall variations in compositions of the ferrotorryweiserite–torryweiserite series (Figure 3a,b) can reflect Ni/Fe and Rh/Ir ratios that vary importantly among droplets of fractionated melt or portions of fluid in various ore deposits. In addition, sulfur fugacities can also be important to control the Ni/Fe ratio, as is known in pentlandite, e.g., [26]. In the Marathon deposit, an increase in oxygen fugacity likely played a major role in the formation of torryweiserite-ferrotorryweiserite via the progressive oxidation of precursor grains of pentlandite and intermediate oberthürite [3].

Author Contributions: The authors wrote the article together. A.Y.B., R.F.M.: data analysis, conclusions, writing; N.D.T.: investigations, discussions, writing; N.T.: synchrotron X-ray micro-Laue diffraction study, writing; A.M.M., L.J.C.: discussions, conclusions, writing. All authors have read and agreed to the published version of the manuscript.

Funding: This research was supported in part by the Russian Science Foundation (grant #22-27-00419).

Data Availability Statement: The data are available upon a reasonable request (from A.Y.B.).

Acknowledgments: This research used beamline 12.3.2 at the Advanced Light Source. A.Y.B. acknowledges that this study was supported in part by the Russian Foundation for Basic Research (project # RFBR 19-05-00181). A support from the Cherepovets State University is gratefully acknowledged (A.Y.B.). N.D.T. also acknowledges that this study was carried out within the framework of the state assignment of the Sobolev Institute of Geology and Mineralogy of the SB of the RAS, financed by the Ministry of Science and Higher Education of the Russian Federation. We appreciate the help of Lang Shi with the electron–microprobe analyses at McGill University. We thank the editorial board members and six anonymous reviewers for their constructive comments.

Conflicts of Interest: The authors declare no conflict of interest.

References

1. Barkov, A.Y.; Tolstykh, N.D.; Tamura, N.; Martin, R.F.; McDonald, A.M.; Cabri, L.J. Ferrotorryweiserite, IMA 2021-055. *CNMNC Newsletter* 64. *Eur. J. Miner.* **2021**, *33*.
2. McDonald, A.M.; Kjarsgaard, I.M.; Bindi, L.; Ross, K.C.; Ames, D.E.; Cabri, L.J.; Good, D.J. Torryweiserite, IMA 2020-048. *CNMNC Newsletter* 58. Copernicus Publications on behalf of the European Mineralogical Societies DMG, SEM, SIMP & SFMC: 2020. Available online: http://cnmnc.main.jp/Newsletter_58_EJM.pdf (accessed on 1 June 2021).
3. McDonald, A.M.; Kjarsgaard, I.; Cabri, L.J.; Ross, K.C.; Ames, D.E.; Bindi, L.; Good, D.J. Oberthürite, $Rh_3(Ni,Fe)_{32}S_{32}$, and torryweiserite, $Rh_5Ni_{10}S_{16}$, two new platinum-group minerals from the Marathon deposit, Coldwell complex, Ontario, Canada: Descriptions, crystal chemical considerations and comments on the geochemistry of rhodium. *Can. Mineral.* **2021**, *59*. in press. [[CrossRef](#)]
4. Ames, D.E.; Kjarsgaard, I.M.; McDonald, A.M.; Good, D.J. Insights into the extreme PGE enrichment of the W horizon, Marathon Cu–Pd deposit, Coldwell alkaline complex, Canada: Platinum-group mineralogy, compositions and genetic implications. *Ore Geol. Rev.* **2017**, *90*, 723–747. [[CrossRef](#)]
5. Barkov, A.Y.; Tolstykh, N.D.; Martin, R.F.; McDonald, A.M. Tamuraite, $Ir_5Fe_{10}S_{16}$, a New Species of Platinum-Group Mineral from the Sisim Placer Zone, Eastern Sayans, Russia. *Minerals* **2021**, *11*, 545. [[CrossRef](#)]
6. Barkov, A.Y.; Tolstykh, N.D.; Tamura, N.; Martin, R.F.; Ma, C. Kuvaevite, IMA 2020-043. *CNMNC Newsletter* 58. Copernicus Publications on behalf of the European Mineralogical Societies DMG, SEM, SIMP & SFMC: 2020. Available online: http://cnmnc.main.jp/Newsletter_58_EJM.pdf (accessed on 1 June 2021).

7. Tolstykh, N.D.; Krivenko, A.P. On the composition of sulfides containing the platinum-group elements. *Zap. Vses. Mineral. Obsh.* **1994**, *123*, 41–49. (In Russian)
8. Barkov, A.Y.; Shvedov, G.I.; Nikiforov, A.A.; Martin, R.F. Platinum-group minerals from Seyba, Eastern Sayans, Russia, and substitutions in the PGE-rich pentlandite and ferhodsites series. *Mineral. Mag.* **2019**, *83*, 531–538. [[CrossRef](#)]
9. Barkov, A.Y.; Shvedov, G.I.; Martin, R.F. PGE-(REE-Ti)-rich micrometer-sized inclusions, mineral associations, compositional variations, and a potential lode source of platinum-group minerals in the Sisim Placer Zone, Eastern Sayans, Russia. *Minerals* **2018**, *8*, 181. [[CrossRef](#)]
10. Cabri, L.J. The platinum-group minerals. In *The Geology, Geochemistry, Mineralogy, Mineral Beneficiation of the Platinum-Group Elements*; Cabri, L.J., Ed.; Canadian Institute of Mining, Metallurgy and Petroleum: Montreal, QC, Canada, 2002; Volume 54, pp. 83–150.
11. Cabri, L.J.; Harris, D.C.; Weiser, T.W. Mineralogy and distribution of platinum-group mineral (PGM) placer deposits of the world. *Explor. Min. Geol.* **1996**, *5*, 73–167.
12. Tamura, N. XMAS: A Versatile Tool for Analyzing Synchrotron X-ray Microdiffraction Data. In *Strain and Dislocation Gradients from Diffraction*; Barabash, R., Ice, G., Eds.; Imperial College Press: London, UK, 2014; pp. 125–155.
13. Aubert, A.J. The Geology and Mineralogy of a Tertiary Buried Placer Deposit, Southern British Columbia. M.Sc. Thesis, University of Alberta, Edmonton, AB, Canada, 1979.
14. Evstigneeva, T.L.; Kudryavtsev, A.S.; Rudashevskiy, N.S. Minerals of platinum group from Yubdo (Ethiopia): New data. *Mineral. Zhurnal* **1992**, *14*, 29–41. (In Russian)
15. Barkov, A.Y.; Tolstykh, N.D.; Shvedov, G.I.; Martin, R.F. Ophiolite-related associations of platinum-group minerals at Rudnaya, western Sayans, and Miass, southern Urals, Russia. *Mineral. Mag.* **2018**, *82*, 515–530. [[CrossRef](#)]
16. Jemetio, J.P.F.; Zhou, P.; Kleinke, H. Crystal structure, electronic structure and thermoelectric properties of $\text{Cu}_4\text{Sn}_7\text{S}_{16}$. *J. Alloys Compd.* **2006**, *417*, 55–59. [[CrossRef](#)]
17. Begizov, V.D.; Zavyalov, E.N. Ferhodsites ($\text{Fe, Rh, Ir, Ni, Cu, Co, Pt}$) $_{9-x}\text{S}_8$ —A new mineral from the Nizhniy Tagil ultramafic complex. *New Data Miner.* **2016**, *51*, 8–11. (In Russian)
18. Gagné, O.C.; Belakovskiy, D.I.; Cámara, F.; Uvarova, Y.; Cabri, L.J. New mineral names. *Am. Mineral.* **2018**, *103*, 828–831. [[CrossRef](#)]
19. Barkov, A.Y.; Nikulin, I.I.; Nikiforov, A.A.; Lobastov, B.M.; Silyanov, S.A.; Martin, R.F. Atypical mineralization involving Pd–Pt, Au–Ag, REE, Y, Zr, Th, U, and Cl–F in the Oktyabrsky deposit, Norilsk complex, Russia. *Minerals* **2021**, *11*, 1193. [[CrossRef](#)]
20. Cabri, L.J.; Criddle, A.J.; Laflamme, J.H.G.; Bearne, G.S.; Harris, D.C. Mineralogical study of complex Pt–Fe nuggets from Ethiopia. *Bull. Mineral.* **1981**, *104*, 508–525. [[CrossRef](#)]
21. Sheng, Y.J.; Hutcheon, I.D.; Wasserburg, G.J. Origin of plagioclase-olivine inclusions in carbonaceous chondrites. *Geochim. Cosmochim. Acta* **1991**, *55*, 581–599. [[CrossRef](#)]
22. Frolova, T.I.; Plechov, P.Y.; Tikhomirov, P.L.; Churakov, S.V. Melt inclusions in minerals of allivalites of the Kuril–Kamchatka island arc. *Geochem. Intern.* **2001**, *39*, 336–346.
23. Andrews, D.R.A.; Brenan, J.M. Phase-equilibrium constraints on the magmatic origin of laurite + Ru–Os–Ir alloy. *Can. Mineral.* **2002**, *40*, 1705–1716. [[CrossRef](#)]
24. Cabri, L.J.; Laflamme, J.H.G.; Stewart, J.M.; Turner, K.; Skinner, B.J. On cooperite, braggite, and vysotskite. *Am. Mineral.* **1978**, *63*, 832–839.
25. Barkov, A.Y.; Fleet, M.E. An unusual association of hydrothermal platinum-group minerals from the Imandra layered complex, Kola peninsula, northwestern Russia. *Can. Mineral.* **2004**, *42*, 455–467. [[CrossRef](#)]
26. Kolonin, G.R.; Orsoev, D.A.; Sinyakova, E.F.; Kislov, E.V. The use of Ni:Fe ratio in pentlandite for estimation of sulfur fugacity during the formation of PGE-bearing sulfide mineralization of the Yoko-Dovyren massif. *Dokl. Earth Sci.* **2000**, *370*, 75–79. (In Russian)